(2)

OFFICE OF NAVAL RESEARCH

Contract N0014-87-K-0495

R&T Code No. 400x026
Technical Report No. 2

Transition State Spectroscopy of Hydrogen Transfer Reactions

by

Daniel M. Neumark

To be published in
"Electronic and Atomic Collisions:
Invited Papers of the XVI ICPEAC"

University of California
Department of Chemistry
Berkeley, CA 94720

November 1, 1989

REPORT DOCUMENTATION PAGE

1a. REPORT SECURITY CLASSIFICATION: Unclassified	1b. RESTRICTIVE MARKINGS: N/A
2a. SECURITY CLASSIFICATION AUTHORITY: N/A	3. DISTRIBUTION/AVAILABILITY OF REPORT: Approved for public release; distribution unlimited
2b. DECLASSIFICATION/DOWNGRADING SCHEDULE: N/A	
4. PERFORMING ORGANIZATION REPORT NUMBER(S): Technical Report No. 2	5. MONITORING ORGANIZATION REPORT NUMBER(S):
6a. NAME OF PERFORMING ORGANIZATION: University of California, Berkeley; 6b. OFFICE SYMBOL (If applicable):	7a. NAME OF MONITORING ORGANIZATION: Office of Naval Research
6c. ADDRESS (City, State and ZIP Code): Chemistry Department, University of California, Berkeley, CA 94720	7b. ADDRESS (City, State and ZIP Code): 800 N. Quincy Street, Arlington, VA 22217
8a. NAME OF FUNDING/SPONSORING ORGANIZATION: Office of Naval Research; 8b. OFFICE SYMBOL (If applicable):	9. PROCUREMENT INSTRUMENT IDENTIFICATION NUMBER: N0014-87-K-0495
8c. ADDRESS (City, State and ZIP Code): 800 N. Quincy St., Arlington, VA 22217	10. SOURCE OF FUNDING NOS. — PROGRAM ELEMENT NO.: / PROJECT NO.: / TASK NO.: / WORK UNIT NO.:
11. TITLE (Include Security Classification): "Transition State Spectroscopy of Hydrogen Transfer Reactions" (Unclassified)	
12. PERSONAL AUTHOR(S): Daniel M. Neumark	
13a. TYPE OF REPORT: Interim Technical; 13b. TIME COVERED: FROM May 89 TO Nov 89	14. DATE OF REPORT (Yr., Mo., Day): 11-29-89; 15. PAGE COUNT: 16
16. SUPPLEMENTARY NOTATION: To be published in "Electronic and Atomic Collisions: Invited Papers of the XVI ICPEAC"	
17. COSATI CODES — FIELD: / GROUP: / SUB GR:	18. SUBJECT TERMS (Continue on reverse if necessary and identify by block number): Negative ion photodetachment; clusters

19. ABSTRACT (Continue on reverse if necessary and identify by block number)

The transition state region for several chemical reactions of the type A + HB → HA + B has been investigated via photodetachment of the stable negative ion AHB^-. The photoelectron spectra of $BrHBr^-$ and $BrHI^-$ show resolved vibrational structure attributable to the transition state region of the Br + HBr and Br + HI reactions, respectively. The photoelectron spectra of IDI^- and the cluster ion $IDI^-(N_2O)$ are compared; these spectra probe different parts of the I + HI potential energy surface. Finally, a high resolution threshold photodetachment spectrum of one of the IHI^- features shows evidence for reactive resonances in the I + HI reaction.

20. DISTRIBUTION/AVAILABILITY OF ABSTRACT: UNCLASSIFIED/UNLIMITED ☒ SAME AS RPT. ☒ DTIC USERS ☐	21. ABSTRACT SECURITY CLASSIFICATION: Unclassified
22a. NAME OF RESPONSIBLE INDIVIDUAL: Dr. David L. Nelson	22b. TELEPHONE NUMBER (Include Area Code): (202) 696-4410; 22c. OFFICE SYMBOL:

DD FORM 1473, 83 APR — EDITION OF 1 JAN 73 IS OBSOLETE.

UNCLASSIFIED
SECURITY CLASSIFICATION OF THIS PAGE

to be published in XVI ICPEAC (plenary lecture)

TRANSITION STATE SPECTROSCOPY OF HYDROGEN TRANSFER REACTIONS

Daniel M. Neumark

Department of Chemistry, University of California, Berkeley, CA 94720

The transition state region for several chemical reactions of the type A + HB → HA + B has been investigated via photodetachment of the stable negative ion AHB$^-$. The photoelectron spectra of BrHBr$^-$ and BrHI$^-$ show resolved vibrational structure attributable to the transition state region of the Br + HBr and Br + HI reactions, respectively. The photoelectron spectra of IDI$^-$ and the cluster ion IDI$^-$(N_2O) are compared; these spectra probe different parts of the I + HI potential energy surface. Finally, a high resolution threshold photodetachment spectrum of one of the IHI$^-$ features shows evidence for reactive resonances in the I + HI reaction.

INTRODUCTION

In a hydrogen transfer reaction of the type A + HB → HA + B, the reactants pass through a short-lived [AHB] collision complex or transition state en route to products. One of the fundamental goals in chemical reaction dynamics is to understand the nature of the potential energy surface on which a reaction occurs in the vicinity of the transition state (the transition state region).[1] This will provide a detailed probe of the interatomic forces which govern chemical bond formation and cleavage in a reaction.

During the last 10-15 years, the most popular approach to this problem has been state-to-state chemistry.[2] In a typical experiment, the product state distribution of a chemical reaction is characterized as completely as possible as a function of reactant initial conditions. For example, one might measure the product angular and internal energy distributions at several reactant collision energies. This information has considerable value in its own right and often provides valuable insight into the mechanism of a reaction. However, the extraction of the properties of the transition state region from these asymptotic measurements is very difficult, even for reactions which have been characterized in detail.

This situation has motivated the development of 'transition state spectroscopy' experiments.[3,4] The goal of these studies is to use spectroscopic means to directly probe the short-lived complex formed in a reaction. The initial experiments in this area were performed by Polanyi, Brooks, and their co-workers in 1980.[5,6] Since then, several techniques involving frequency and time-domain spectroscopy have been applied to this problem.[7-15] However, the short-lived nature of the transition state has limited the successful application of these methods to a relatively small number of systems.

We have developed an

alternative approach to the spectroscopy of the transition state in bimolecular reactions. [16-19] We study the unstable [AHB] complex formed in the A + HB hydrogen transfer reaction by photodetaching the stable, hydrogen-bonded negative ion AHB^-. If the ion geometry is similar to that of the neutral transition state, then photodetaching the ion will probe the transition state region of the A + HB potential energy surface. Even though the [AHB] complex is unstable, the photoelectron spectrum of AHB^- can exhibit resolved vibrational structure which yields considerable insight into the spectroscopy and dissociation dynamics of the [AHB] complex. Hydrogen transfer reactions are particularly appealing because, in many cases, the [AHB] transition state for the reaction has good geometric overlap with the strongly hydrogen-bonded ion AHB. In addition, most hydrogen transfer reactions are 'heavy + light-heavy' reactions, in which a hydrogen atom is transferred between two much heavier species. The dissociation dynamics of the [AHB] complex with this mass combination favors the observation of resolved vibrational structure in the AHB^- photoelectron spectrum. In essence, we observe the fast vibrational motion of the light H atom as the complex slowly dissociates.

This experiment provides a high degree of control over important parameters of a chemical reaction. Photodetachment initiates the A + HB reaction with the atoms in the same geometry as they are in the ion AHB^-, thereby providing excellent control over the reactant orientation. In addition, since the ions are generated in a source which produces rotationally cold species, we can limit the total angular momentum available to the reaction. The latter restriction is particularly significant since it facilitates comparison with theoretical simulations of our results.

The simplest reactions amenable to this technique are those in which a hydrogen atom is exchanged between two identical halogen atoms. Consider the reaction

$$Br + HBr \rightarrow HBr + Br, \quad (1)$$

which is studied by photodetaching $BrHBr^-$.[19] This ion is predicted to be a linear and centrosymmetric species with an interbromine equilibrium distance $R_e = 3.43 \pm 0.1$ Å.[20,21] Model potential energy surfaces for the Br + HBr reaction[22,23] predict a linear minimum energy path with a barrier < 10 kcal/mol. Thus, reasonable geometric overlap is expected between the ion and neutral transition state.

We have also studied simple asymmetric reactions[24] such as

$$Br + HI \rightarrow HBr + I, \quad (2)$$

as well as more complex reactions involving polyatomic reactants[18] such as

$$F + CH_3OH \rightarrow HF + CH_3O. \quad (3)$$

Finally, the photoelectron spectra of cluster ions such as $IDI^-(N_2O)$ have been obtained as a first step towards understanding what happens when a reaction is initiated by photodetaching a cluster of known size. Reactions (1) and (2) will be discussed below, along with the cluster ion results. Results obtained with a higher resolution

instrument on the I + HI reaction will also be discussed.

EXPERIMENTAL

Two types of negative ion photodetachment experiments are used in this work. The instruments used in these experiments are described in detail elsewhere.

Most of the results to date were obtained with 'fixed-frequency' negative ion photoelectron spectroscopy.[25,26] Our apparatus is a time-of-flight photoelectron spectrometer similar to that described in Ref. 26. Internally cold negative ions are generated by crossing a pulsed, free-jet expansion of an appropriate mixture of gases with a 1 keV electron beam. The ions are mass-selected via time-of-flight and photodetached with a pulsed, fixed-frequency laser. The data shown below were taken using either the 4th or 5th harmonic of a Nd:YAG laser at 266 nm (4.66 eV) or 213 nm (5.82 eV), respectively. The kinetic energy of the ejected photoelectrons is determined with a time-of-flight analyzer. The resolution of the energy analyzer is 5-8 meV at low electron kinetic energy (0.5 - 0.6 eV), but this degrades approximately as $E^{3/2}$ at higher electron kinetic energy.

Higher resolution studies were performed on a threshold photodetachment spectrometer.[27] This instrument has a similar ion source to the fixed-frequency apparatus and also uses time-of-flight mass selection. However, the ions are photodetached with a tunable pulsed dye laser. At a given laser wavelength, only electrons produced with nearly zero-kinetic energy are detected. The zero-kinetic energy spectrum plotted as a function of laser wavelength consists of a series of peaks, each corresponding to an ion→neutral transition. The width of the peaks is determined by the ability of the instrument to discriminate against photoelectrons produced with high kinetic energy. By adapting the methods developed by Schlag and co-workers for threshold photoionization of neutrals,[28] we have achieved a resolution of 3 cm^{-1} (0.37 meV) with this instrument. In the experiments performed with this instrument (Section 4, below), tunable laser light in the range of 300 nm was required. This was obtained by frequency doubling the output of an excimer pumped dye laser in a β-barium borate crystal. The laser repetition rate was 50 Hz. With Rhodamine B as the dye, 2 mJ/pulse of frequency-doubled light was obtained.

RESULTS AND DISCUSSION

1) $BrHBr^-$ Photoelectron Spectrum

The photoelectron spectra of $BrHBr^-$ and $BrDBr^-$ taken at 213 nm are shown in Figure 1. The spectra are discussed and analyzed in considerable detail in Ref. 19; only the salient features are summarized here. Each spectrum shows several resolved peaks of varying widths. In these spectra, the electron kinetic energy E is given by

$$E = h\nu - E^-_b - E^0_{int} + E^-_{int}. \quad (4)$$

Here $h\nu$ = 5.82 eV is the photon energy, E^-_b = 4.27 eV[29,30] is the binding energy of the electron to $BrHBr^-$, that is, the energy

necessary to remove an electron from the ground state of $BrHBr^-$ to form Br + HBr(v=0), and E^-_{int} and E^0_{int} are the internal energies of the ion and neutral [BrHBr] complex, respectively. E^-_{int} is measured relative to Br + HBr(v=0). Equation (4) shows that if $E^-_{int} = 0$, then the peaks in a photoelectron spectrum at lower electron kinetic energy correspond to higher values of internal energy in the complex. Note that all the peaks occur at electron kinetic energies less than $h\nu - E^-_b = 1.55$ eV. This is the electron kinetic energy that would result from forming Br + HBr(v=0) from ground state $BrHBr^-$. Hence, the observed peaks in each spectrum correspond to states of the complex that lie above Br + HBr(v=0), that is, states of the complex which can dissociate.

The three peaks at highest electron kinetic energy in the $BrHBr^-$ spectrum are approximately evenly spaced, suggesting a vibrational progression. This is confirmed by the $BrDBr^-$ spectrum, in which the highest energy peak is unchanged, but the spacing between the four highest energy peaks is considerably less than in the $BrHBr^-$ spectrum. This isotope shift indicates that we are observing a vibrational progression of the [BrHBr] complex in a mode primarily involving H atom motion. The progression is assigned to the ν_3 antisymmetric stretch mode, in which the H atom vibrates between the two essentially stationary halogen atoms. Since the highest energy peak occurs at the same energy in the two spectra, it is assigned to the $\nu_3'' = 0 \rightarrow \nu_3' = 0$ ion $\rightarrow$ neutral transition. There is no evidence for 'hot band' transitions in the spectrum originating from excited ν_3'' levels of the ion. The ν_3 mode is not totally symmetric, so only even ν_3' levels of the neutral are accessible from the $\nu_3'' = 0$ level of the ion. The peaks in this progression in the two spectra are labelled by their ν_3' quantum number. The broad peaks at lower electron energy labelled A' and B' are assigned to an excited electronic state of the [BrHBr] complex and are discussed in more detail in Ref. 19.

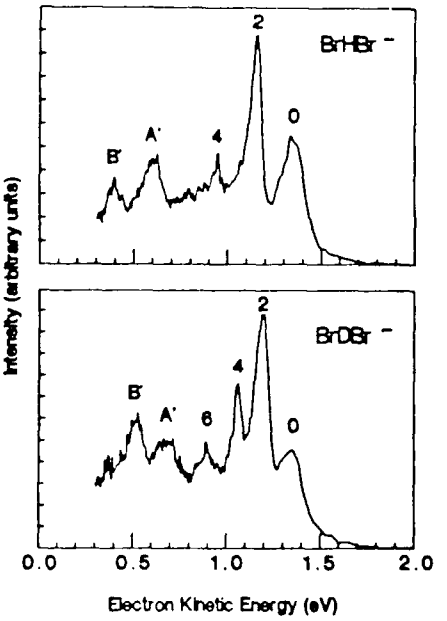

Figure 1. Photoelectron spectra of $BrHBr^-$ and $BrDBr^-$ obtained at 213 nm.

An important feature of these spectra is that the spacing between

necessary to remove an e tron from the ground st HBr⁻ to form Br + HBr(v=(int and E^0_{int} are the interm er s of the ion and neutral [nplex, respectively. E_{int} is mc ed relative to Br + HBr(Equation (4) shows that if E), hen the peaks in a photoel n s ectrum at lower electron kine energy correspond to higher values of internal energy in the co lex. Note that all the peaks c r at electron kinetic energies s than hν - E_b = 1.55 eV T the electron kinetic en would result from forming Br Br(v=0) from ground state BrHBr⁻ Hence, the observed peaks in eac spectrum correspond to states of the complex that lie above Br + H (v=0), that is, states of the comple which can dissociate.

The three peak highest electron kinetic energy in the BrHBr⁻ spectrum are ap ximately evenly spaced, suggesting a vibrational progression. This is confirmed by the BrDBr⁻ sp ectrum, in which he highest energ peak is unchanged, but the spacing between the four highest energ ks is considerably ss than e BrHBr⁻ spectrum. This isot pe s ft indicates that we are obtai ing a vibrational progression of the [BrHBr] complex in a mode primarily involving H motion. The progression is assigne to the ν_3 antisymmetric stretch mod , in which the H atom vibra between the two essentially s ry halogen atoms. Si ighest energy peak occurs ame energy in the two sp t is assigned to the $\nu_3'' = 0 \rightarrow \nu_3' = 0$ ion → neutral transition. The e is no evidence for 'hot band' tra sitions in the sp ctrum originating fr m excited ν_3'' levels of the ion. The ν_3 mode is not totally symmetric, so only even ν_3' levels of the neutral are accessible from the $\nu_3'' = 0$ level of the ion. The peaks in this progression in the two spectra are labelled by their ν_3' quantum number. The broad peaks at lower electron energy labelled A' and B' are assigned to an excited electronic state of the [BrHBr] complex and are discussed in more detail in Ref. 19.

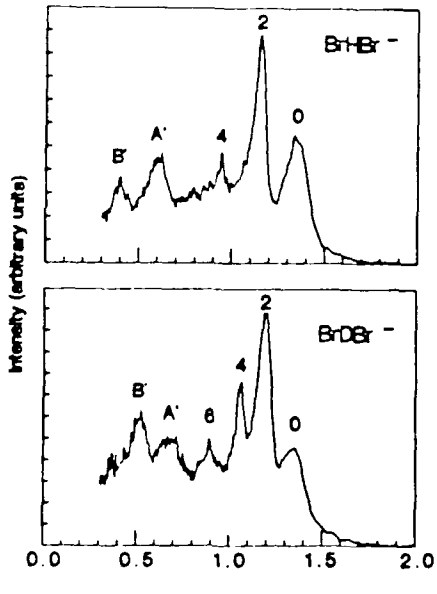

Figure 1. Photoelectron spectra of BrHBr⁻ and BrDBr⁻ obtained at 213 nm.

An important feature of these spectra is that the spacing between

the peaks in the ν_3 progression is considerably less than the vibrational frequency in diatomic HBr. The $\nu_3' = 0$ and $\nu_3' = 2$ peaks in the $BrHBr^-$ spectrum are separated by 1700 cm^{-1}, while the HBr fundamental is at 2560 cm^{-1}. This shows that our experiment probes the transition state region of the Br + HBr potential energy surface where the H atom is expected to interact strongly with both Br atoms. In effect, we are probing the region of the surface where the strong bond in diatomic HBr has been replaced by two weak bonds in the [BrHBr] complex.

In a heavy + light-heavy reaction such as Br + HBr, the ν_3 mode of the [BrHBr] complex in the transition state region is poorly coupled to dissociation of the complex. Thus, although the peaks in the photoelectron spectra correspond to states of the [BrHBr] complex with enough energy to dissociate, they correspond to a progression in a vibrational mode which is not the dissociation coordinate of the complex. Similar effects have been seen in electronic spectra involving transitions to dissociative states of polyatomic molecules.

The peaks widths in the $BrHBr^-$ and $BrDBr^-$ spectra are a measure of the dissociation dynamics of the [BrHBr] complex. The peaks become progressively narrower as ν_3' increases; the $\nu_3' = 0$ peak in the $BrHBr^-$ spectrum is 150 meV wide, whereas the $\nu_3' = 4$ peak is only 20 meV wide. This is at first glance a counter-intuitive result; it implies that states of the complex with higher internal energy (in the ν_3 mode) have longer lifetimes. However, previous calculations on heavy + light-heavy reactions[31] predict the existence of levels of the complex which are quasi-bound along the dissociation coordinate (the symmetric stretch coordinate in this case) and which become more pronounced for more highly excited antisymmetric stretch levels of the complex. These quasi-bound states are responsible for the sharp resonance structure[32] observed in reactive scattering calculations on these systems. The narrow $\nu_3' = 4$ peak in the $BrHBr^-$ spectrum and $\nu_3' = 6$ peak in the $BrDBr^-$ spectrum are assigned to transitions to these quasi-bound [BrHBr] levels.

The ultimate goal of this experiment is to learn about the Br + HBr potential energy surface in the vicinity of the transition state. This is done by constructing a flexible functional form for the Br + HBr potential energy surface and varying the parameters of the surface until the $BrHBr^-$ and $BrDBr^-$ photoelectron spectra are successfully reproduced in spectral simulations. The accurate simulation of these spectra requires calculating the Franck-Condon overlap between the ion vibrational wavefunction and the three-dimensional scattering wavefunctions supported by the Br + HBr surface over a wide energy range. These calculations have been performed by Schatz[33] and Bowman[34] on a model Cl + HCl surface in order to simulate the $ClHCl^-$ photoelectron spectrum. Miller[35] has done this type of calculation on a model F + H_2 surface in a simulation of the FH_2^- photoelectron spectrum. However, these calculations are too complex to use in our iterative analysis. We have therefore developed an approximate method to simulate our spectra.

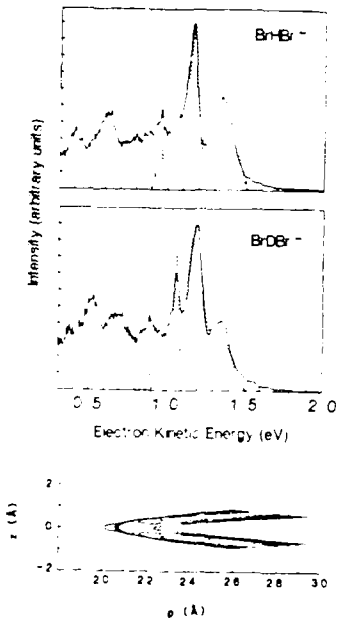

Figure 2. (bottom) Best-fit 'effective collinear potential energy surface for Br + HBr reaction. Shaded area shows region that has best Franck-Condon overlap with ground state of $BrHBr^-$.
(top) Simulations of ground state progressions in the $BrHBr^-$ and $BrDBr^-$ spectra superimposed on the experimental spectra.

We construct an 'effective' collinear potential energy surface[36] which is a collinear Br + HBr surface with the zero-point bending energy of the [BrHBr] complex implicitly included at every point. The surface that provides the best fit to our spectra is shown at the bottom of Figure 2. The shaded region shows the part of the surface which has good Franck-Condon overlap with the ground state of $BrHBr^-$. The simulations of the spectra are very sensitive to small changes in this region (the Franck-Condon region) of the surface. This region of the surface plays a key role in the dynamics of the Br + HBr reaction. The simulated spectra obtained with this surface are shown superimposed on the experimental spectra at the top of Figure 2. We see that reasonable agreement is obtained between experimental and simulated peak positions, intensities, and widths for the ground state progression.

In summary, the photoelectron spectra of $BrHBr^-$ and $BrDBr^-$ are a sensitive probe of the transition state region of the Br + HBr potential energy surface. The peaks in the spectra reveal the spectroscopy and dissociation dynamics of the [BrHBr] complex, and strongly suggest the existence of reasonably long-lived (approximately 100 fs) quasi-bound levels of the complex. The spectra have been analyzed to yield an approximate potential energy surface for the reaction.

2) $BrHI^-$ Photoelectron Spectrum

The transition state region for the reaction Br + HI → HBr + I is accessible through photodetachment of the asymmetric bihalide ion $BrHI^-$. The $BrHI^-$ and $BrDI^-$ photoelectron spectra taken at 213 nm are shown in Figure 3. Each spectrum shows two progressions of evenly spaced peaks. The peak widths are between 100-150 meV. The origins of the two progressions occur at the same electron energies

in each spectra, and the peak spacing within each progression is noticeably smaller in the $BrDI^-$ spectrum. Each progression is assigned to the ν_3 mode of the [BrHI] complex. The two progressions in each spectrum are assigned to two electronic states of the complex. The splitting between the origins of the progressions is 7300 cm^{-1}, which is very close to the splitting between the $^2P_{3/2}$ ground state and the $^2P_{1/2}$ spin-orbit excited state of atomic iodine. Hence the progression at higher electron energy is assigned to the ground electronic state of the [BrHI] complex, while the progression at lower electron energy is likely due to an excited state of the complex which correlates asymptotically to $HBr + I^*(^2P_{1/2})$.

The scale at the top of Figure 3 shows that the peak spacing in both progressions in the $BrHI^-$ spectrum is only slightly less than the vibrational frequency in diatomic HBr. This is in sharp contrast to the much larger 'red shift' seen in the $BrHBr^-$ spectrum. One can understand this result by considering the geometry of the $BrHI^-$ ion. The proton affinity of Br^- is 0.47 eV higher than that of I^-. Hence, the H atom in the ion should be significantly closer to the Br atom; the ion can be pictured as I^-·HBr. This means that photodetachment of the ion will primarily access the I + HBr product valley on the neutral potential energy surface. In this region, the nascent HBr bond is nearly complete. We therefore expect to observe a vibrational frequency in the photoelectron spectrum characteristic of this nearly-formed bond, which is indeed the experimental result.

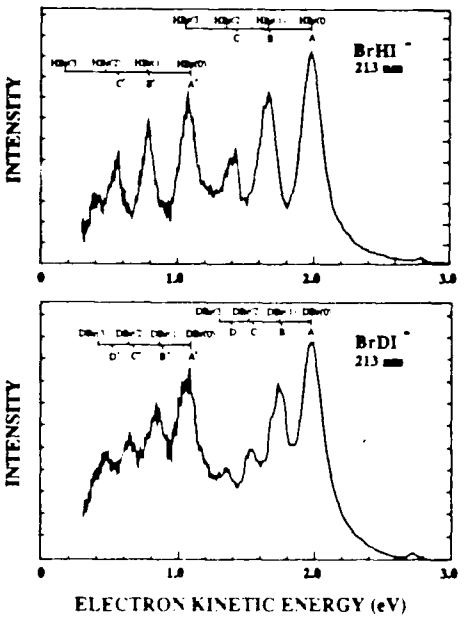

Figure 3. $BrHI^-$ and $BrDI^-$ photoelectron spectra obtained at 213 nm.

We have simulated the ground state progression in the $BrHI^-$ spectrum using the time-dependent wave-packet formalism developed by Heller,[37] Kosloff,[38] and others.[39,40] A model potential energy surface proposed by Broida and Persky[41] for the Br + HI reaction is used in the simulations. This surface is of the London-Eyring-Polanyi-Sato (LEPS) functional form.[42] The procedure for estimating the $BrHI^-$ potential energy surface is described by us elsewhere. This is a two-dimensional simulation restricted to

collinear geometries.

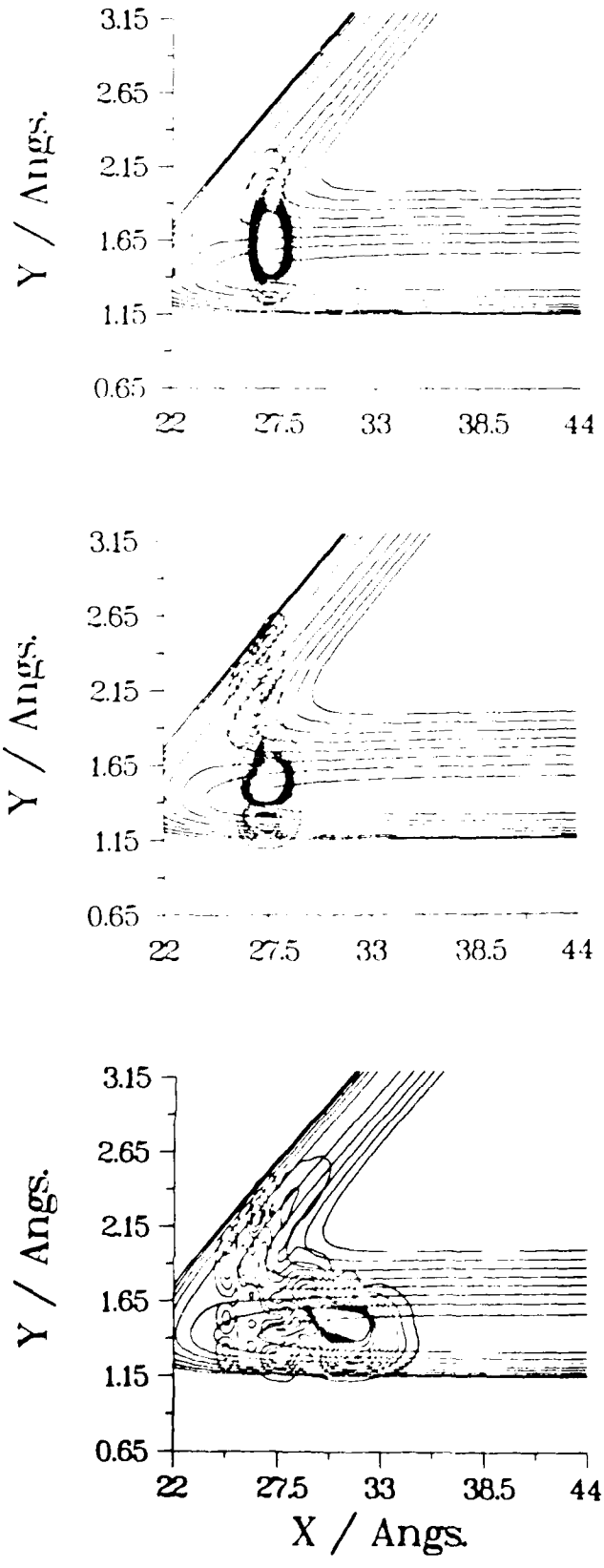

Figure 4. Wavepackets at t=0 (top), t = 40 fs (middle), and t = 160 fs (bottom), on Br + HI potential energy surface resulting from $BrHI^-$ photodetachment. The surface is plotted using the mass-scaled coordinates $y = R_{H\text{-}Br}$ and $x = (\mu_{I,HBr}/\mu_{HBr})^{1/2}(R_{I\text{-}Br})$.

The procedure is as follows. The initial wavepacket $\psi(0)$ on the Br + HI surface is obtained by projecting the ion ground state wavefunction onto the neutral surface, assuming the Franck-Condon principle is valid. This wavepacket is then propagated in time on the reactive surface using the method described by Kosloff and Kosloff.[36a] The autocorrelation function $C(t) = \langle\psi(0)|\psi(t)\rangle$ is calculated, and the Fourier transform of C(t) yields the simulated photoelectron spectrum.

Figure 4 shows the initial wavepacket on the Br + HI surface, as well as the wavepacket at the later times t=40 fs and t=160 fs. Figure 5 shows a plot of $|C(t)|$, and the simulated spectrum is superimposed on the experimental spectrum in Figure 6. Figure 4 shows that the initial wavepacket is localized in the I + HBr product valley as discussed above. The plot at t= 160 fs shows that photodetachment of $BrHI^-$ leads primarily to I + HBr products; very little of the wavepacket ends up in the Br + HI valley.

The plot of the autocorrelation function provides some interesting physical insight into our experiment. The most prominent feature in Figure 5 is a high-frequency oscillation which is damped after about 30 fs. This high frequency motion is the ν_3 mode of the [BrHI] complex, and the rapid decay of this

oscillation is due to dissociation of the complex. The frequency of the oscillation determines the peak spacing in the photoelectron spectrum, while the time scale for decay determines the peak widths. Thus the structure in the $BrHI^-$ photoelectron spectrum shows the [BrHI] complex vibrating along the ν_3 coordinate as it falls apart.

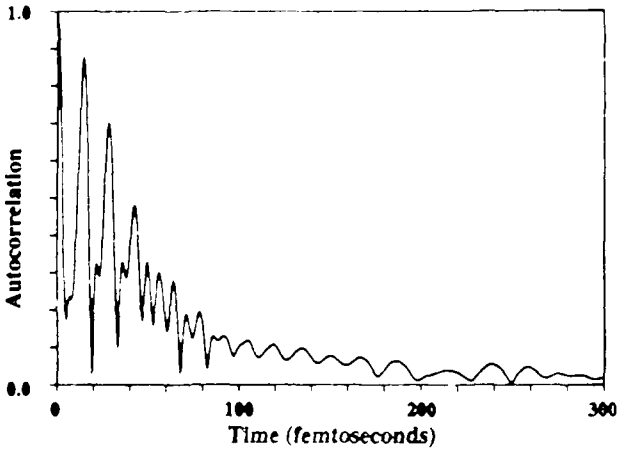

Figure 5. Modulus of autocorrelation function |C(t)| vs. t for propagation of wavepacket shown at top of Figure 4.

The simulated spectrum shows four nearly evenly spaced peaks and a small, partly resolved clump of peaks at 1.20 eV. The positions of the first three peaks agree reasonably well with the three highest energy peaks in the experimental spectrum, although the simulated widths are too narrow. The overly narrow widths may result from deficiencies in the LEPS surface used in the simulations. A surface which is more repulsive in the I + HBr valley will yield broader peaks in the simulated photoelectron spectrum. In addition, if the minimum energy path on the true surface were bent, then a more accurate simulation not restricted to collinear geometries would probably yield broader peaks.

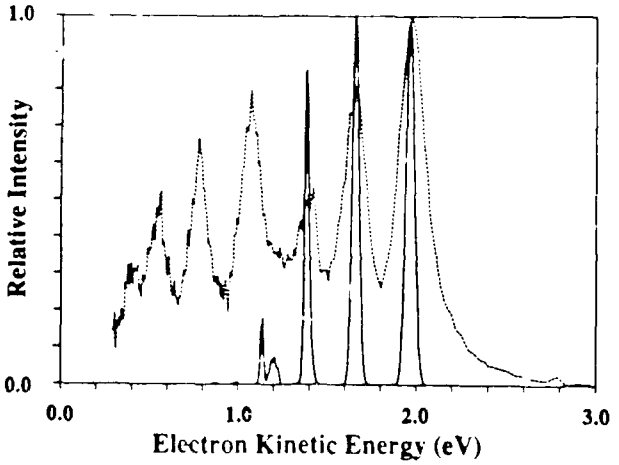

Figure 6. Simulated $BrHI^-$ photoelectron spectrum obtained from Fourier transform of C(t) of Figure 5 superimposed on experimental spectrum. Only the ground state progression was modelled.

The clump of peaks in the simulation at 1.2 eV is from transitions to a series of [BrHI] resonances supported by the LEPS surface localized largely in the Br +

HI reactant valley. The contribution from these states can be seen in Figure 5; they lead to the persistence of $|C(t)|$ at long times. Due to the low intensity of these transitions in the simulation, our experiment does not completely rule out their existence. We therefore cannot say if a more accurate potential energy surface would support these resonances.

3) $IDI^-(N_2O)$ Photoelectron Spectrum

The photoelectron spectroscopy of negative cluster ions has become a very active research field in recent years.[43-47] This class of experiments, particularly those of Bowen and co-workers,[43b] has led us to pursue a new direction in our own efforts. Suppose we measure the photoelectron spectrum of a cluster ion in which a bihalide ion is surrounded by a known number of solvating species, i.e. $IDI^-(S)_n$. There is no ambiguity concerning the number of solvating species since the ions are mass-selected prior to photodetachment. Photodetachment of the cluster ion generates a neutral collision complex surrounded by the solvating species; such an experiment may serve as a probe of condensed phase reaction dynamics. As a first step to studying larger clusters, we have obtained the photoelectron spectrum of $IDI^-(N_2O)$, shown in Figure 7 below the photoelectron spectrum of the bare IDI^- ion. These spectra were taken at 266 nm.

A comparison of the two spectra indicates that the addition of an N_2O molecule has perturbed but not destroyed the structure seen in the IDI^- spectrum. Both spectra show three peaks. These are assigned to even members of the ν_3

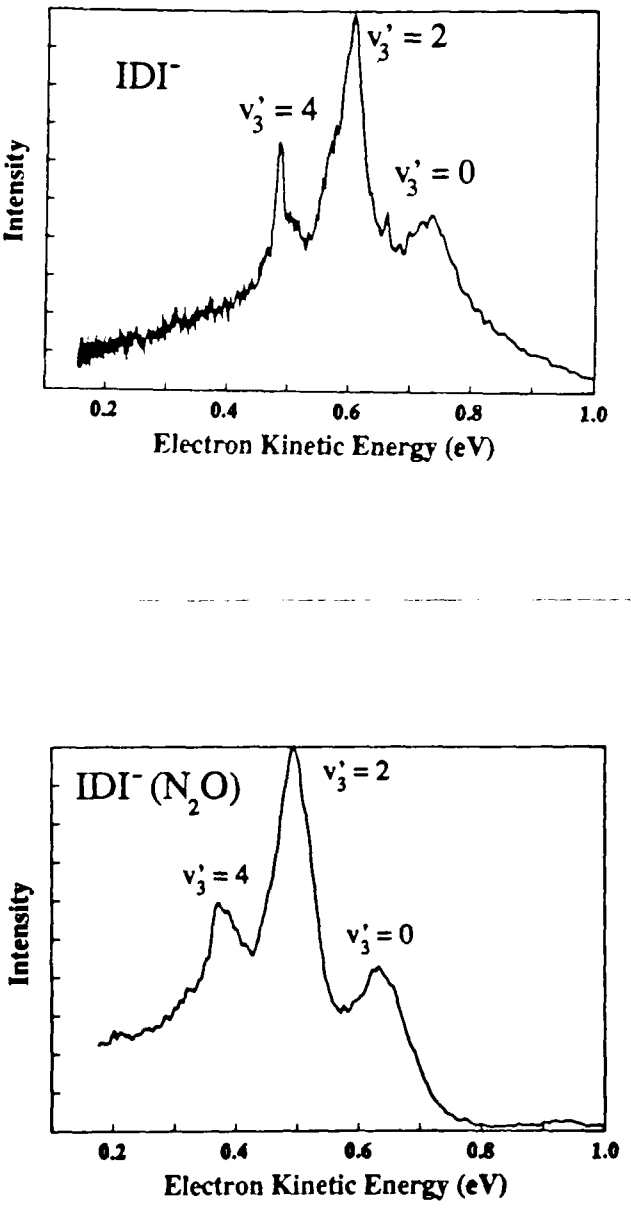

Figure 7. Photoelectron spectrum of IDI^- (top) and $IDI^-(N_2O)$ (bottom) taken at 266 nm.

progression in the neutral complex just as in the $BrHBr^-$ spectrum. The 0→0 transition is shifted toward lower electron energy by 0.100 eV in the cluster ion spectrum. Assuming that N_2O interacts much more strongly with IDI^- than with the [IDI] complex, then this shift yields the binding energy of N_2O with IDI^-. Shifts of this magnitude were seen in Bowen's photoelectron spectroscopy study of the series NO^-, $NO^-(N_2O)$, and $NO^-(N_2O)_2$.[43b]

A important difference between the bare and clustered IDI^- spectra is that the spacing between the three peaks is slightly different. The $\nu_3' = 0$ and $\nu_3' = 2$ peaks are more widely spaced by 0.013 eV in the $IDI^-(N_2O)$ spectrum, and the $\nu_3' = 2$ and $\nu_3' = 4$ spacing is 0.007 eV less than in the bare ion spectrum. These differences are small but significant and were not seen in Bowen's spectra of the NO^- series. We believe this variation in the peak spacing results because photodetachment produces an unstable collision complex rather than a stable molecule in our experiment.

A plausible explanation for our observation is as follows. In the cluster ion $IDI^-(N_2O)$, some charge transfer is expected from the IDI^- ion to the N_2O molecule. This can distort the IDI^- geometry, most likely by lengthening the interiodine distance since the extra electron is what holds the ion together in the first place. On the other hand, subsequent to photodetachment, it is a reasonable approximation to ignore the interaction between the [IDI] complex and neighboring N_2O molecule. Thus, the cluster ion photoelectron spectrum is, to first order, equivalent to the photoelectron spectrum of slightly distorted IDI^-.

Figure 8 shows a model collinear potential energy surface for the I + HI reaction.[48] The horizontal and vertical axes are proportional to the symmetric and antisymmetric stretch normal coordinates, respectively. In our earlier work on the IDI^- photoelectron spectrum,[17] we estimated the equilibrium interiodine distance in IDI^- to be R_e = 3.88 Å. This distance corresponds to the dashed vertical line drawn through the surface in Figure 8. A cut through the surface at this interiodine distance yields a double minimum potential which is, to a good approximation, the antisymmetric stretch potential for the [IDI] complex with an interiodine distance of 3.88 Å. This potential is shown in Figure 9a, along with the eigenvalues for the first few even ν_3' levels. Suppose that the interiodine distance in $IDI^-(N_2O)$ is 0.05 Å greater than in the bare ion. The antisymmetric stretch potential for the [IDI] complex for this geometry is obtained by taking the cut through the surface indicated by the dotted line in Figure 8. This potential and its first few even eigenvalues are shown in Figure 9b. The major difference between the two potentials is that the barrier between the two minima is higher at larger interiodine distance. While this pushes up all the eigenvalues, the $\nu_3' = 2$ level is the most strongly affected since it lies very close to the barrier. The result is that in the antisymmetric stretch potential associated with the cluster ion, the $\nu_3' = 0$ and $\nu_3' = 2$ levels are further apart, and the $\nu_3' = 2$ and $\nu_3' = 4$ levels are closer together. This is consistent with the

experimentally observed peak spacings.

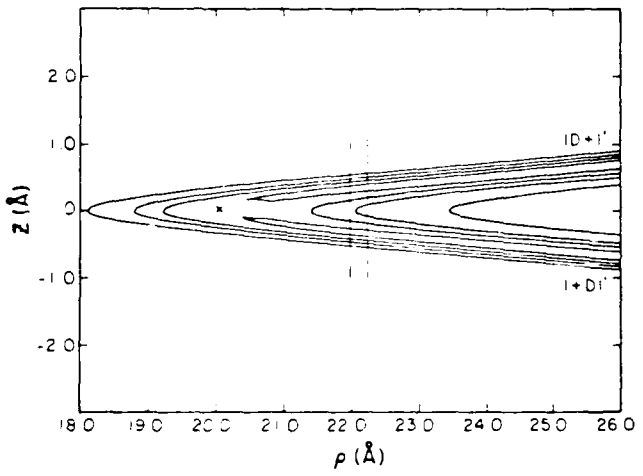

Figure 8. Model collinear potential energy surface for I + DI reaction. Solid vertical line corresponds to estimated interiodine distance R_e = 3.88 Å in IDI^-. The dashed vertical line corresponds to estimated R_e = 3.93 Å in $IDI^-(N_2O)$.

Thus, our simple picture qualitatively explains the experimental results. The photoelectron of a cluster ion such as $IDI^-(N_2O)$ allows one to probe different regions of the I + DI potential energy surface and also gives an indication of the nature of the interaction in the cluster ion. We plan to study the photoelectron spectra of similar cluster ions in the near future as a function of the type and number of solvating species.

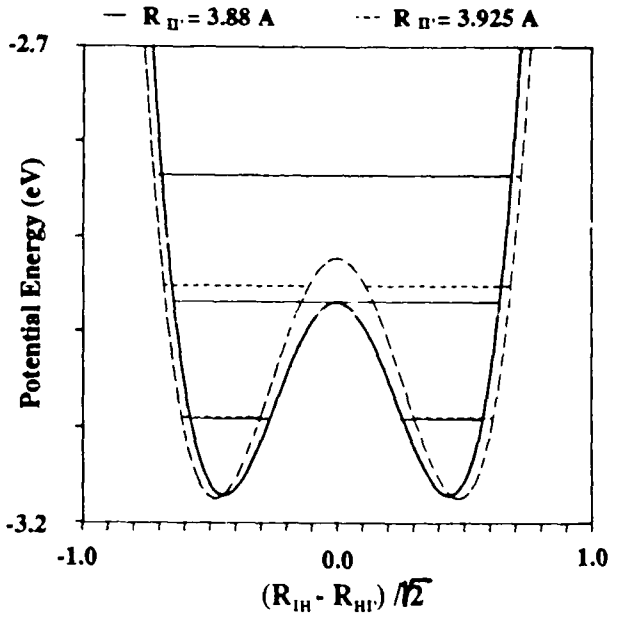

Figure 9. Antisymmetric stretch potentials and ν_3 = 0, 2, and 4 energy levels for [IDI]complex obtained by cuts through I + HI potential energy surface at interiodine distances of 3.88 Å (solid lines) and 3.93 Å (dashed lines).

4) Threshold Photodetachment Spectrum of IHI^-

Figure 10 shows the IHI^- photoelectron spectron previously obtained by us.[17] The I + HI reaction is predicted to exhibit the most pronounced resonance effects due to quasi-bound IHI states supported by the potential energy surface.[31,49] This results from both

the large m_I/m_H mass ratio and the low barrier expected for the reaction. Simulations of the IHI^- photoelectron spectrum[17,34,50] predict that some of the ν_3' peaks should exhibit underlying structure at higher resolution due to a progression in quasi-bound symmetric stretch levels of the [IHI] complex; these levels are quasi-bound along the dissociation coordinate of the complex. These simulations were performed on a model LEPS surface for the I + HI reaction on which the barrier is probably too low. Nonetheless, the prediction of more structure under the peaks in the IHI^- photoelectron spectrum prompted an investigation of this system with our threshold photodetachment spectrometer[27] which, as discussed above, has considerably higher resolution than the 'fixed-frequency' instrument used to obtain the the spectrum in Figure 10.

Figure 11 shows a scan of the $\nu_3' = 2$ peak (the middle peak in Figure 10) obtained with the threshold photodetachment spectrometer. This spectrum shows three partly resolved peaks which decrease in intensity toward lower wavelength. The peaks are spaced by about 100 cm^{-1}. This is in the range expected for the symmetric stretch frequency for quasi-bound states of the [IHI] complex. Although the narrow peaks in the $BrHBr^-$ and $BrDBr^-$ spectra were assigned to resonances, the observation of this low frequency progression in the IHI^- threshold photodetachment spectrm provides even more compelling evidence for the existence of these quasi-bound levels. The observation of these levels is of considerable interest not only because it confirms long-standing theoretical predictions, but because it also provides more detailed spectroscopic information on the transition state region of the I + HI potential energy surface. Further investigation of the IHI^- threshold photodetachment spectrum is currently in progress in order to substantiate the claim that we are observing [IHI] resonances. We plan to take high resolution spectra of the other ν_3' peaks in the IHI^- and IDI^- photoelectron spectra in order to determine which of them, if any, exhibit underlying structure. Meanwhile, the spectrum in Figure 11 can be regarded as very promising result.

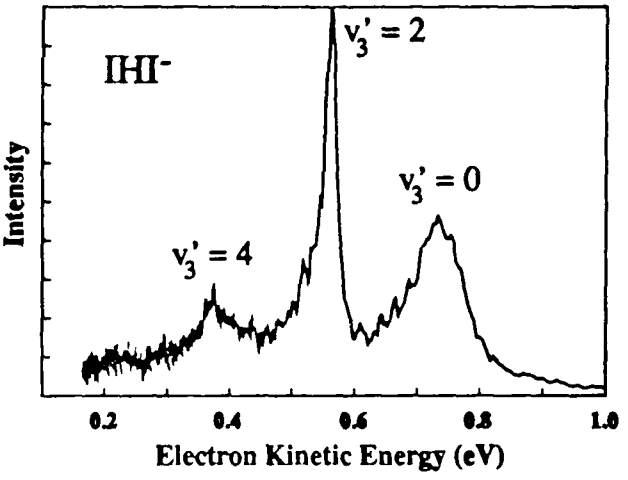

Figure 10. Photoelectron spectrum of IHI^- taken at 266 nm.

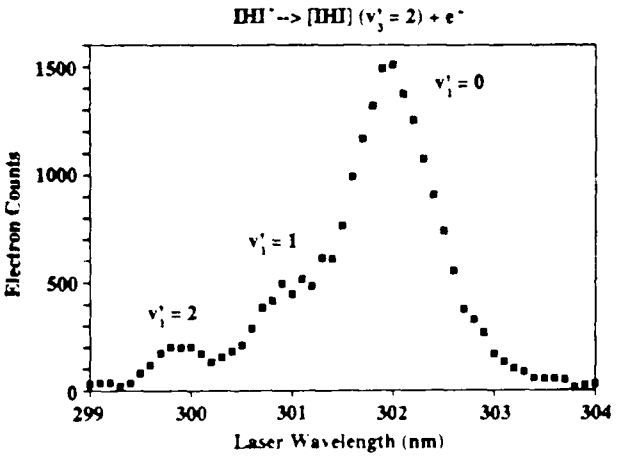

Figure 11. Threshold photodetachment spectrum of [IHI] ν_3 = 2 peak.

SUMMARY

Negative ion photodetachment can provide a detailed probe of the transition state region of a chemical reaction. The examples above show the application of this method to several simple reactions. Future directions include the investigation of more complex chemical reactions, reactions initiated by photodetaching a cluster ion (Section 3, above), and higher resolution studies with our threshold photodetachment spectrometer (Section 4, above).

ACKNOWLEDGMENTS

The photoelectron spectroscopy work is supported by the Air Force Office of Scientific Research under Grant No. AFOSR-87-0341. The threshold photodetachment studies are supported by the Office of Naval Research Young Investigator Program under Grant No. N0014-87-K-0495.

The results shown here were obtained with the aid of my postdoctoral fellow, Dr. Irene Waller, and my graduate students Don Arnold, Steven Bradforth, Doug Cyr, Theo Kitsopoulos, Jennifer Loeser, Ricardo Metz, and Alexandra Weaver.

REFERENCES

1. R. D. Levine and R. B. Bernstein, Molecular Reaction Dynamics and Chemical Reactivity (Oxford University Press, New York, 1987), pp. 396-510.

2. S. R. Leone, Annu. Rev. Phys. Chem. **35**, 109 (1984).

3. P. R. Brooks, Chem. Rev. **88**, 407 (1988).

4. A. H. Zewail, Science **242**, 1645 (1988).

5. P. Arrowsmith, F. E. Bartoszek, S. H. P. Bly, T. Carrington, Jr., P. E. Charters, and J. C. Polanyi, J. Chem. Phys. **73**, 5895 (1980).

6. P. Hering, P. R. Brooks, R. F. Curl, Jr., R. S. Judson, and R. S. Lowe, Phys. Rev. Lett. **44**, 687 (1980); T. C. Maguire, P. R. Brooks, R. F. Curl, J. H. Spence, and S. J. Ulvick, J. Chem. Phys. **85**, 844 (1986).

7. H. P. Grieneisen, H. Xue-jing, and K. L. Kompa, Chem. Phys. Lett.

82, 421 (1981).

8. P. D. Kleiber, A. M. Lyyra, K. M. Sando, V. Zafiropulos, and W. C. Stwalley, J. Chem. Phys. **85**, 5493 (1986).

9. A. Benz and H. Morgner, Molec. Phys. **57**, 319 (1986).

10. B. A. Collings, J. C. Polanyi, M. A. Smith, A. Stowlow, and A. W. Tarr, Phys. Rev. Lett. **59**, 2551 (1987).

11. J.-C. Nieh and J. J. Valentini, Phys. Rev. Lett. **60**, 519 (1988).

12. S. Buelow, G. Radhakrishnan, J. Catanzarite, and C. Wittig, J. Chem. Phys. **83**, 444 (1985).

13. W. H. Breckenridge, C. Jouvet, and B. Soep, J. Chem. Phys. **84**, 1443 (1986).

14. D. G. Imre, J. L. Kinsey, R. W. Field, and D. H. Katayama, J. Phys. Chem. **86**, 2564 (1982).

15. M. Dantus, M. J. Rosker, and A. H. Zewail, J. Chem. Phys. **87**, 2395 (1987); R. M. Bowman, M. Dantus, and A. H. Zewail, Chem. Phys. Lett. **156**, 131, (1989).

16. R. B. Metz, T. Kitsopoulos, A. Weaver, and D. M. Neumark, J. Chem. Phys. **88**, 1463 (1988).

17. A. Weaver, R. B. Metz, S. E. Bradforth, and D. M. Neumark, J. Phys. Chem. **92**, 5558 (1988).

18. S. E. Bradforth, A. Weaver, R. B. Metz, and D. M. Neumark, Advances in Laser Science - IV Proceedings of the 1988 International Laser Science Conference (in press).

19. R. B. Metz, A. Weaver, S. E. Bradforth, T. N. Kitospoulos, and D. M. Neumark, J. Phys. Chem. (in press- to be published 2/90).

20. B. J. Ault, Acc. Chem. Res. **15**, 103 (1982).

21. A. B. Sannigrahi and S. D. Peyerimhoff, J. Mol. Struct. **165**, 55 (1988).

22. I. Last and M. Baer, J. Chem. Phys. **80**, 3246 (1983).

23. J. M. White and D. L. Thompson, J. Chem. Phys. **61**, 719 (1974).

24. S. E. Bradforth, A. Weaver, D. W. Arnold, and D. M. Neumark, manuscript in preparation.

25. D. G. Leopold, K. K. Murray, and W. C. Lineberger, J. Chem. Phys. **81**, 1048 (1984);

26. L. A. Posey, M. J. DeLuca, and M. A. Johnson, Chem. Phys. Lett. **131**, 170 (1986)

27. T. N. Kitsopoulos, I. M. Waller, J. G. Loeser, and D. M. Neumark, Che. Phys. Lett. **159**, 300 (1989).

28. K. Muller-Dethlefs, M. Sander, and E. W. Schlag, Z. Naturforsch. **39a**, 1089 (1984).

29. H. Hotop and W. C. Lineberger, J. Phys. Chem. Ref. Data, **14**, 731 (1985).

30. G. Caldwell and P. Kebarle, Can. J. Chem. **63**, 1399 (1985).

31. E. Pollak, J. Chem. Phys. **78**,

1228 (1983); D. K. Bondi, J. N. L. Connor, J. Manz, and J. Romelt, J. Mol. Phys. **50**, 467 (1983).

32. D. G. Truhlar and A. Kuppermann, J. Chem. Phys. **52**, 3841 (1970); S.-F. Wu and R. D. Levine, Mol. Phys. **22**, 881 (1971).

33. G. C. Schatz, J. Chem. Phys. **90**, 3582 (1989).

34. J. M. Bowman and B. Gazdy, J. Phys. Chem. **93**, 5129 (1989); B. Gazdy and J. M. Bowman, J. Chem. Phys. (in press).

35. J. Zhang and W. H. Miller, J. Chem. Phys. (submitted).

36. J. M. Bowman, Adv. Chem. Phys. **61**, 115 (1985).

37. E. J. Heller, J. Chem. Phys. **68**, 3891 (1978); Acc. Chem. Res. **14**, 368 (1981).

38. D. Kosloff and R. Kosloff, J. Comput. Phys. **52**, 35 (1983); R. Kosloff and D. Kosloff, J. Chem. Phys. **79**, 1823 (1983); R. Kosloff, J. Phys. Chem. **92**, 2087 (1988).

39. R. H. Bisseling, R. Kosloff, and J. Manz, J. Chem. Phys. **83**, 993 (1985).

40. N. E. Henriksen, J. Zhang, and D. G. Imre, J. Chem. Phys. **89**, 5607 (1988).

41. M. Broida and A. Persky, Chem. Phys. **133**, 405 (1989).

42. S. Sato, Bull. Chem. Soc. Jpn., **28**, 450 (1955).

43. J. V. Coe, J. T. Snodgrass, C. B. Friedhoff, K. M. McHugh, and K. H. Bowen, J. Chem. Phys. **83**, 3169 (1985); J. Chem. Phys. **87**, 4302 (1987).

44. D. G. Leopold, J. Ho, and W. C. Lineberger, J. Chem. Phys. **86**, 1715 (1987).

45. O. Cheshnovsky, S. H. Yang, C. L. Pettiette, Y. Liu, and R. E. Smalley, Chem. Phys. Lett. **138**, 119 (1987).

46. M. J. Deluca, B. Niu, and M. A. Johnson, J. Chem. Phys. **88**, 5857 (1988).

47. G. Gantefor, K. H. Meiwes-Broer, and H. O. Lutz, Phys. Rev. Lett. **37**, 2716 (1988).

48. J. Manz and J. Romelt, Chem. Phys. Lett. **81**, 179 (1981).

49. J. Manz, R. Meyer, and H. H. R. Schor, J. Chem. Phys. **80**, 1562 (1984).

50. G. C. Schatz, J. Chem.Phys. **90**, 4847 (1989).